BMC Physiology

Research article

Blockade of maitotoxin-induced oncotic cell death reveals zeiosis

Mark Estacion[1] and William P Schilling*[1,2]

Address: [1]Rammelkamp Center for Education and Research, MetroHealth Medical Center, Cleveland, OH, USA and [2]Department of Physiology and Biophysics, Case Western Reserve University School of Medicine, Cleveland, OH, USA

E-mail: Mark Estacion - mestacion@metrohealth.org; William P Schilling* - wschilling@metrohealth.org

*Corresponding author

Published: 10 January 2002

BMC Physiology 2002, **2**:2

Received: 20 November 2001

Accepted: 10 January 2002

This article is available from: http://www.biomedcentral.com/1472-6793/2/2

Abstract

Background: Maitotoxin (MTX) initiates cell death by sequentially activating 1) Ca^{2+} influx via non-selective cation channels, 2) uptake of vital dyes via formation of large pores, and 3) release of lactate dehydrogenase, an indication of cell lysis. MTX also causes formation of membrane blebs, which dramatically dilate during the cytolysis phase. To determine the role of phospholipase C (PLC) in the cell death cascade, U73122, a specific inhibitor of PLC, and U73343, an inactive analog, were examined on MTX-induced responses in bovine aortic endothelial cells.

Results: Addition of either U73122 or U73343, prior to MTX, produced a concentration-dependent inhibition of the cell death cascade ($IC_{50} \approx 1.9$ and 0.66 μM, respectively) suggesting that the effect of these agents was independent of PLC. Addition of U73343 shortly after MTX, prevented or attenuated the effects of the toxin, but addition at later times had little or no effect. Time-lapse videomicroscopy showed that U73343 dramatically altered the blebbing profile of MTX-treated cells. Specifically, U73343 blocked bleb dilation and converted the initial blebbing event into "zeiosis", a type of membrane blebbing commonly associated with apoptosis. Cells challenged with MTX and rescued by subsequent addition of U73343, showed enhanced caspase-3 activity 48 hr after the initial insult, consistent with activation of the apoptotic program.

Conclusions: Within minutes of MTX addition, endothelial cells die by oncosis. Rescue by addition of U73343 shortly after MTX showed that a small percentage of cells are destined to die by oncosis, but that a larger percentage survive; cells that survive the initial insult exhibit zeiosis and may ultimately die by apoptotic mechanisms.

Background

Recent studies have shown that maitotoxin (MTX), a potent cytolytic agent isolated from the dinoflagellate *Gambierdiscus toxicus*, is an important new molecular tool for the study of oncotic (necrotic) cell death [1,2]. In a variety of cell types, MTX initiates a cell death cascade that involves a sequence of cellular events essentially identical to those activated by stimulation of purinergic receptors of the P2Z/$P2X_7$ type. Initially, MTX causes a graded increase in cytosolic free Ca^{2+} concentration ($[Ca^{2+}]_i$). This is followed closely in time by the opening of cytolytic/oncotic pores (COP) that allow the exchange of large organic molecules of molecular weight less than ~800 Daltons across the plasma membrane. COP activation can be monitored by the cellular accumulation of ethidium or propidium-based vital dyes, which are normally excluded from the cytoplasm, but gain access to cellular nucleotides via COP and exhibit an increase in fluorescence. In isolated bovine

aortic endothelial cells (BAECs), the opening or activation of COP is associated with formation of spherical membrane blebs with a diameter of 3–5 microns [3]. The final stage of MTX-induced cell death is cell lysis as indicated by the release of large cytoplasmic enzymes, such as lactate dehydrogenase (LDH). Using time-lapse videomicroscopy, we have shown that MTX-induced release of LDH from vascular endothelial cells is associated with massive bleb dilation and rapid staining of the nucleus with vital dyes [3].

The initial MTX-induced increase in $[Ca^{2+}]_i$ reflects the activation of a Ca^{2+}-permeable non-selective cation channel (CaNSC) [1,4–8]. This channel, which has a reported conductance in the range of 12–40 pS depending on ionic conditions [5,9–11], causes rapid membrane depolarization, which in excitable cells, leads to activation of voltage-sensitive channels. Although it appears that a rise in $[Ca^{2+}]_i$ is necessary, but not sufficient for activation of COP [1], the molecular mechanisms by which this occurs remains unknown. Likewise, the subsequent steps leading to membrane blebbing and cytolysis are poorly understood. It is however, well established that MTX causes the hydrolysis of phosphoinositides in some cell types, presumably via activation of phospholipase C (PLC) [12,13]. Activation of PLC by MTX appears to be indirect resulting as a consequence of increased $[Ca^{2+}]_i$. These results suggest that PLC may be involved in activation of COP and/or in the cytolysis phase of MTX action. Thus, the initial purpose of the present study was to determine the role of PLC in MTX-induced cell death. To accomplish this goal, the effect of U73122, a specific inhibitor of mammalian PLC was examined. This compound selectively inhibits mammalian PLC, but has no direct effect on bacterial PLC, bacterial or mammalian phospholipase A_2 or adenylyl cyclase [14]. U73343, a structural analogue of U73122 that differs by only one double bond, has no direct effect on PLC and is commonly used as a negative control. However, both compounds have been shown to produce non-specific effects presumably unrelated to inhibition of PLC [15–20]. The results of the present study show, that both U73122 and U73343 inhibit MTX-induced change in $[Ca^{2+}]_i$, ethidium uptake, and LDH release in BAECs. Although these results suggest that blockade of MTX-induced responses by the U-compounds is independent of PLC, they identify these compounds as novel, potent, and rapid blockers of MTX action. Interestingly, in experiments designed to examine MTX reversibility, we discovered a rather stunning change in the pattern of membrane blebbing. Specifically, cells rescued from MTX by subsequent application of U73343 exhibit a blebbing pattern known as "zeiosis". Zeiosis, which comes from the Greek word *Ζειω* meaning "to boil over" [21], is characterized by violent cytokinesis with continuous bleb extension and retraction. Zeiosis has been associated in many cell types with apoptosis [22–24]. The results of the present experiments suggest that following a brief exposure to MTX, U73343 rescues cells from oncotic cell death. Cells that survive the initial insult may ultimately die by apoptosis.

Results

U73122 and U73343 inhibit MTX-induced change in $[Ca^{2+}]_i$ and ethidium uptake in BAECs.

To test the hypothesis that MTX-induced cell death requires PLC, the effect of U73122, a specific inhibitor of PLC was examined. Addition of MTX to fura-2 -loaded BAECs, suspended in a cuvette in normal Ca^{2+}-containing buffer at 37°C, produced a time-dependent increase in $[Ca^{2+}]_i$ (Fig 1, *upper panel*). Addition of either U73122 or U73343, the inactive analog, ~3 min before MTX produced a concentration-dependent inhibition of the change in $[Ca^{2+}]_i$. U73343 exhibited a 3-fold greater potency compared to U73122 (Fig 1, *insets*). Since U73343 has no significant effect on PLC over the concentration range employed [14,25–27], these results suggest that inhibition of the MTX-induced response is independent of PLC.

Studies in BAECs have shown that following elevation of $[Ca^{2+}]_i$, MTX causes the activation of large pores (i.e., COP) that allow the flux of ethidium and propidium-based vital dyes into the cell. As previously reported [3], MTX-induced uptake of ethidium in BAECs was biphasic in the absence of the U-compounds (Fig 1, *lower panel*). The first phase, which extends for ~5 min after addition of MTX, reflects the activation of COP, whereas the second phase is temporally associated with LDH release and thus reflects cell lysis [3]. Addition of either U73122 or U73343, ~3 min before MTX, produced an inhibition of ethidium uptake (Fig 1, *lower panel*). Both phases of ethidium uptake were attenuated by the U-compounds and U73343 again appeared to have a greater potency compared to U73122. These results suggest that inhibition of MTX-induced change in $[Ca^{2+}]_i$ prevents or attenuates both the activation of COP and cytolysis.

To determine if the effects of the U-compounds are reversible, BAECs were pre-treated with U73343 (5 μM) for 5 min, washed and resuspended in normal extracellular buffer in the absence of U73343. As seen in Fig 2, BAECs pre-treated with U73343 partially recover responsiveness to MTX following washout of U73343, but the response failed to recover further over the subsequent 10 min. Thus, the ability of U73343 to block the effect of MTX appears to reflect both a rapidly reversible and slowly reversible component.

U73343 partially reverses the effect of MTX.

To determine if U73343 could reverse the action to MTX, the compound was added to the cuvette after MTX. As

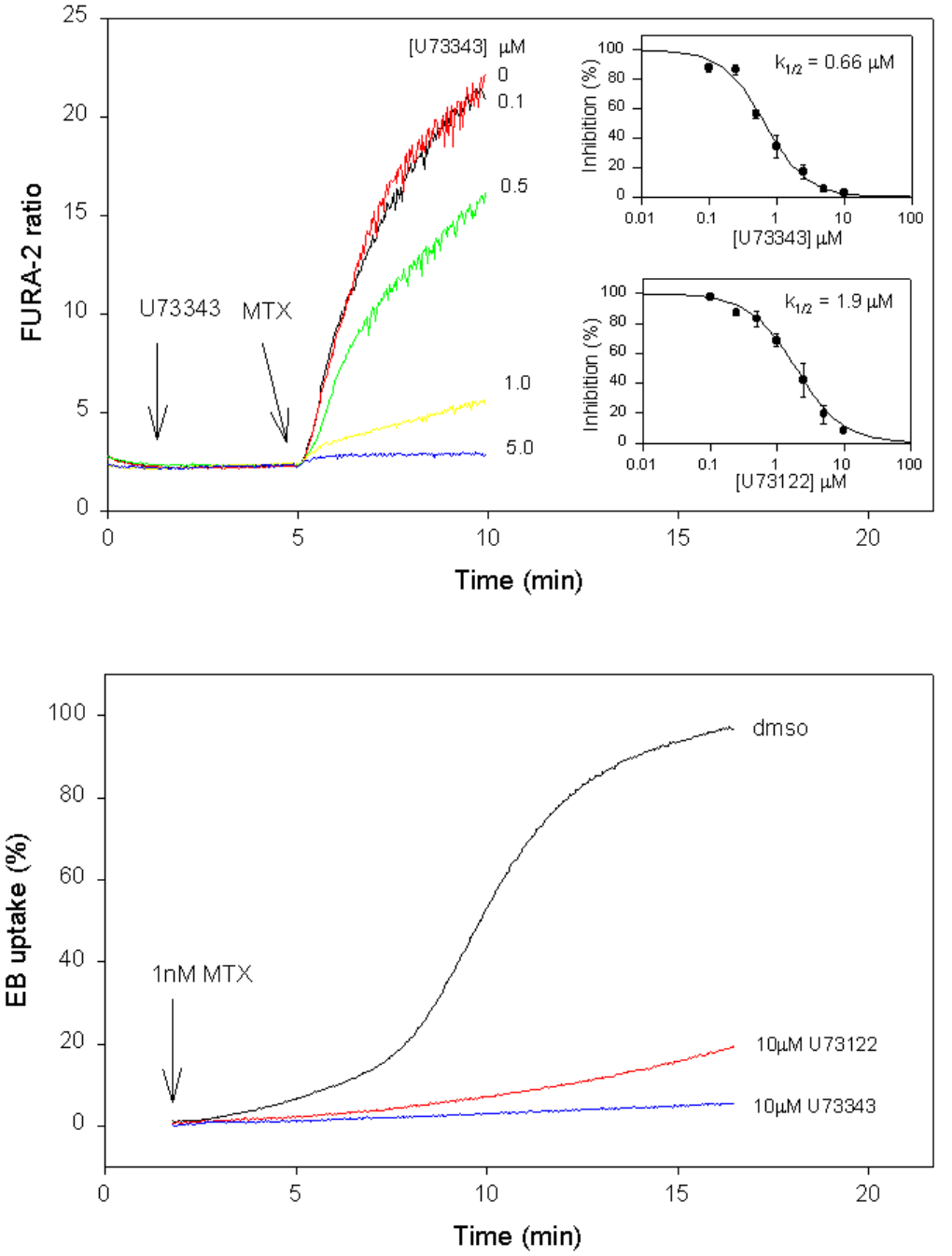

Figure 1
U73343 and U73122 block MTX-induced Ca^{2+} influx and ethidium uptake. *Upper panel.* Fura-2 loaded BAECs were suspended in HBS and the fluorescence ratio was recorded as a function of time. Five traces are shown superimposed. At time 100 sec, U73343 was added at the final concentration indicated to the right of each trace. At time 300 sec 0.3 nM MTX was added to stimulate Ca^{2+} influx. Concentration-response curves were determined for both U73122 (n = 3) and U73343 (n = 5). Inset shows the % inhibition relative to DMSO control. *Lower panel.* Ethidium bromide (EB) uptake in BAECs was determined from the increase in fluorescence as a function of time as described in *Materials and Methods.* U73122 (red trace), U73343 (blue trace), or DMSO (black trace) were added at time 0, EB was added at 50 sec, and MTX was added at 200 sec. Values shown are normalized to the maximum fluorescence obtained by addition of digitonin at the end of each trace. Results shown are representative of 3 independent experiments.

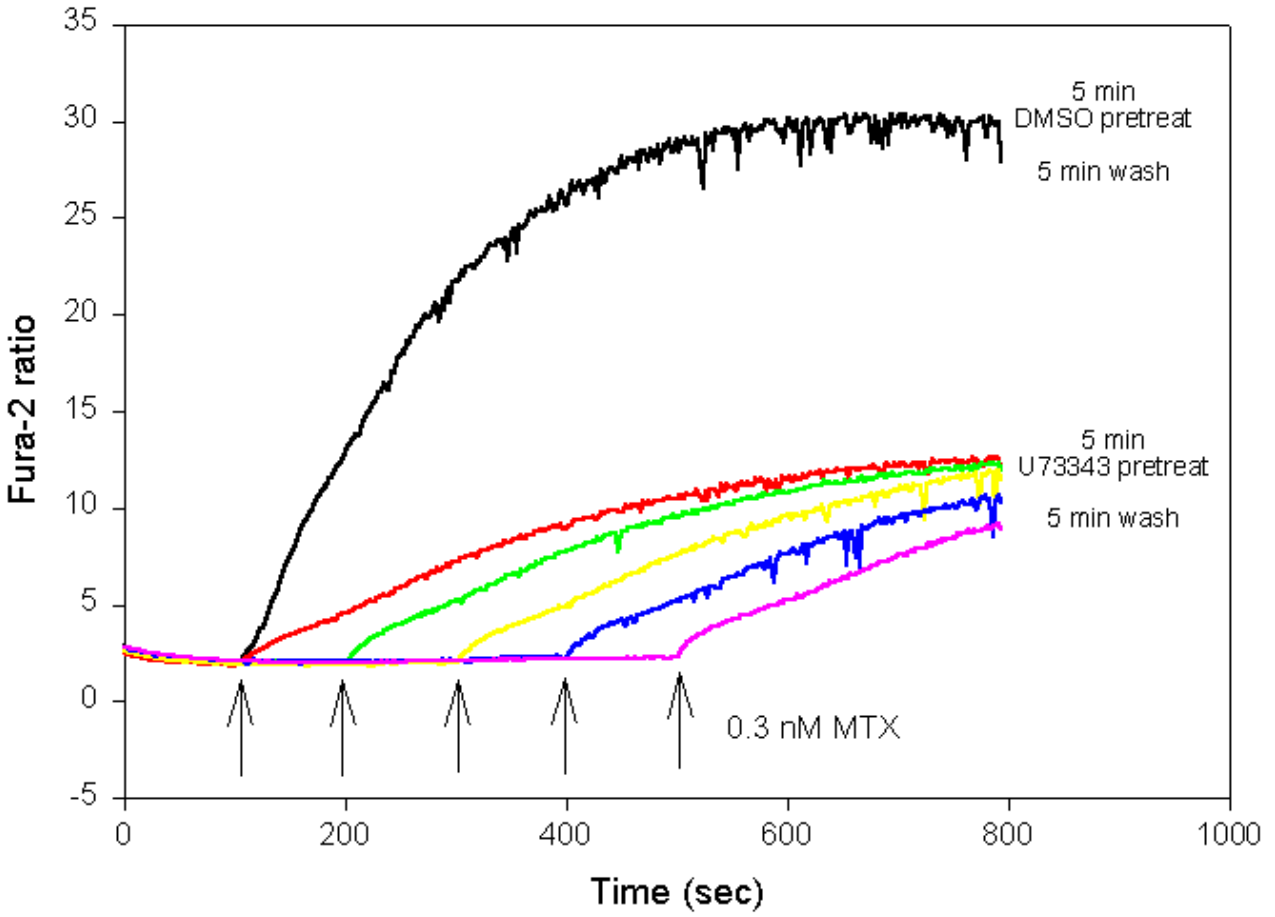

Figure 2
Blockade of MTX-induced Ca^{2+} influx by U73343 is partially reversible. Prior to fluorescence recording, fura-2 loaded BAECs were equilibrated with HBS containing either 5 μM U73343 or 0.1% DMSO for 5 min. The cells were washed to remove the drug which required ~5 min. The cells were resuspended in the absence of U73343, immediately placed in a cuvette, and the fluorescence recorded. Addition of 0.3 nM MTX at 100 sec to the DMSO-treated cells (black trace) resulted in a typical MTX response. Addition of MTX to the U73343 pretreated cells at 100 (red), 200 (green), 300 (yellow), 400 (blue) or 500 sec (purple) are shown superimposed. Results shown are representative of 3 independent experiments.

seen in Fig 3 (*upper panel*), addition of U73343 at various times after MTX, immediately stopped further increases in $[Ca^{2+}]_i$ and resulted in an immediate recovery of $[Ca^{2+}]_i$ back towards basal resting levels. Over the time-course examined however, $[Ca^{2+}]_i$ never fully returned to the level observed before MTX addition. The same experimental protocol was employed for evaluation of ethidium uptake (Fig 3, *lower panel*). Again, MTX-induced uptake of ethidium was biphasic in the absence of U73343 (*trace a*). Addition of the U-compound shortly after MTX (i.e., at 200 sec; *trace e*), blocked both phases of the response. Addition of U73343 towards the end of the first phase (i.e., at either 400 or 500 sec; *traces b* and c) had only a small effect on the magnitude and time course of subsequent ethidium uptake. However, when U73343 was added during the first phase of ethidium uptake (i.e., 300 sec; *trace d*), dye accumulation in the cells was immediately blocked. After a short delay, dye uptake again increased with time to a value that was substantially less than maximum. These results suggest that U73343 is able to rapidly block both the MTX-induced change in $[Ca^{2+}]_i$ and COP formation when added shortly after MTX. When U73343 is added at longer times, a large proportion of the cells challenged by MTX have apparently passed a point-of-no-return and are destined to die by oncosis. However, the percentage of cells that either die or survive depends on the time of U73343 addition after MTX.

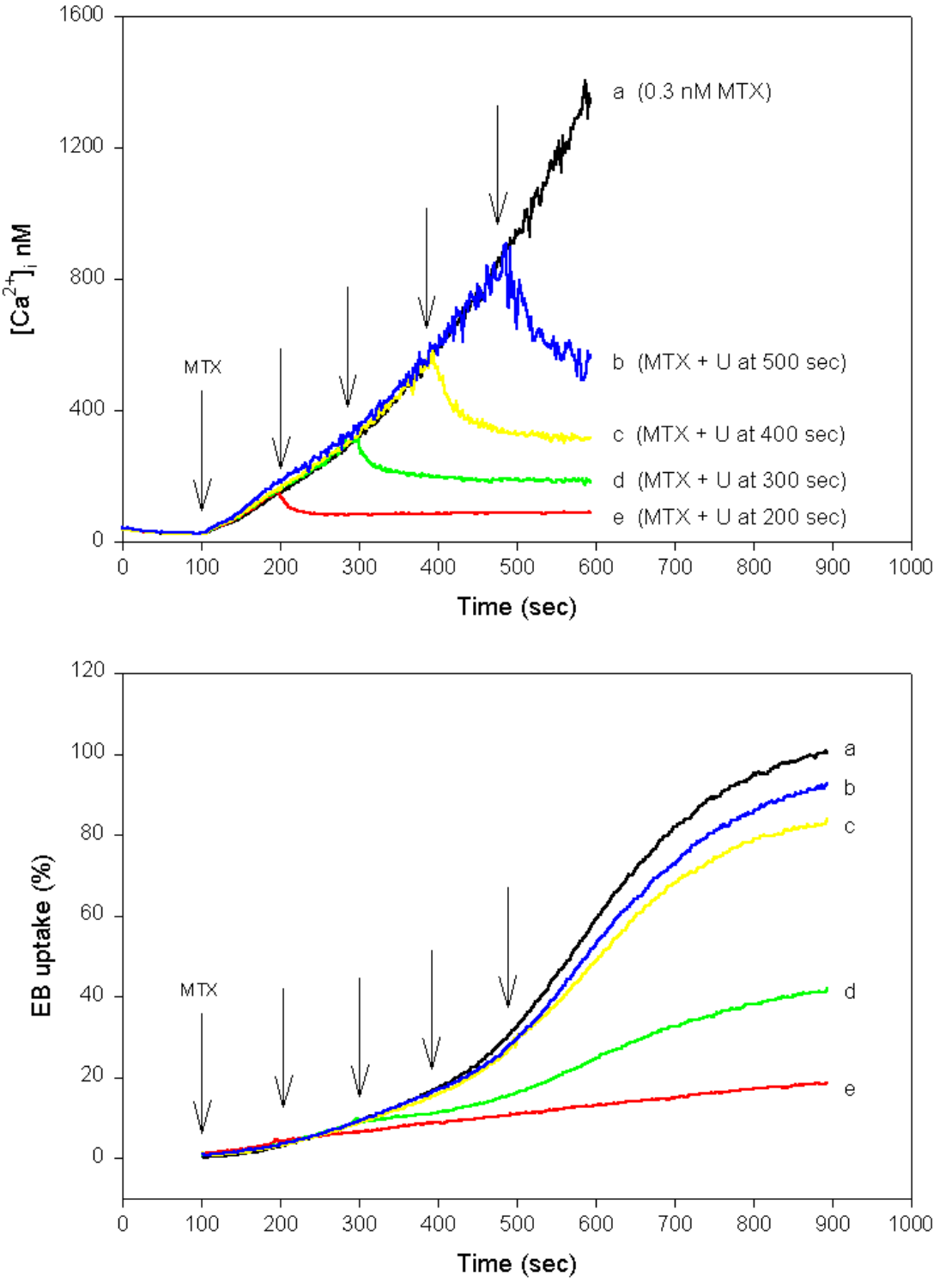

Figure 3
U73343 rapidly blocks and partially reverse the effects of MTX. Five traces are shown superimposed in each panel. *Upper panel.* Fura-2 loaded BAECs were stimulated with MTX at 100 sec. U73343 (5 μM) was subsequently added at either 200 (red), 300 (green), 400 (yellow), or 500 sec (blue). *Lower panel.* EB uptake in BAECs with the same protocol and trace colors as the upper panel are shown. Results shown are representative of 3 independent experiments.

U73343 rescues cells from MTX-induced oncotic cell death.

To directly determine the effect of U73343 on MTX-induced cell lysis, LDH release was correlated with the change in $[Ca^{2+}]_i$ and ethidium uptake in paired experiments. As previously reported [3] and as seen in Fig. 4 (*bottom panel, black circles*), MTX-induced LDH release in the absence of U73343, correlates in time with the second phase of ethidium uptake, demonstrating that the second phase reflects cell lysis. Addition of U73343 during the first phase of the MTX-induced response, immediately reversed the rise in $[Ca^{2+}]_i$ and blocked dye uptake. However, at ~400 sec, ethidium uptake resumed and increased to an intermediate value as was seen in Fig 3. This secondary uptake of ethidium correlated in time with a partial LDH release (Fig 4, *bottom panel, red triangles*). U73343 alone had no effect on LDH release (Fig 4, *bottom panel, green squares*). These results directly demonstrate that a percentage of cells within the population died by oncosis, but perhaps more importantly, that a significant number of the cells are rescued from MTX-induced oncotic cell death when U73343 is added within a short time-window after MTX.

U73343 alters MTX-induced bleb formation.

Our previous studies showed that MTX causes a specific change in cell morphology. In particular, MTX causes dramatic time-dependent membrane blebbing in BAECs [3]. An example is shown in Fig. 5. BAECs, attached to glass coverslips and superfused with a solution containing ethidium bromide, were simultaneously monitored by phase and fluorescence microscopy. Selected images pairs (merged phase/fluorescence images) are shown in Fig 5. At time 5 min, the cells were superfused with a solution containing MTX. No change in cell morphology was noted at 10 min, but by 25 min (i.e., 20 min after addition of MTX) large membrane blebs were observed on essentially all the cells within the field of view (Fig 5A, see examples indicated by *blue arrows*). Additionally, clear staining of the nucleus and cytoplasm by ethidium was observed at this time. The graph shown in Fig 5A quantifies the fluorescence change in individual cells as a function of time. Note that uptake of ethidium in response to MTX is biphasic at the single cell level and that heterogeneity between cells primarily reflects the time of entry into the second phase of dye uptake, i.e., the cell lysis phase. The dynamic nature of the MTX-induced bleb formation, bleb dilation, and ethidium uptake can be observed by viewing the time-lapse movie associated with this experiment (see Additional File 1). As previously reported, blebs form during the first phase of dye uptake, whereas rather dramatic bleb dilation is seen during the cytolysis phase of rapid dye uptake. In the continuous presence of MTX, blebs continue to swell and in many cases seem to disappear as they dilate and extend out of the focal plane.

Addition of U73343 (10 μM) 2–3 min before MTX (0.3 nM) completely blocks ethidium uptake and the associated change in cell morphology. As seen in Fig 5B, essentially no blebs are observed at 25 min (i.e., 20 min after MTX) and little or no dye uptake is seen out to 40 min. Thus, the major morphological changes associated with MTX challenge are blocked by U73343. However, by time 40 min, some of the cells (11 out of 53) detach from the glass coverslip and round-up (Fig 5B, see examples indicated by *blue arrows*). The time-lapse movie of this experiment revealed that these detached cells were actually undergoing a novel type of membrane blebbing called zeiosis (see Additional File 2). As can be seen from the movie (Additional File 2), zeiosis is characterized by cytokinesis with time-dependent bleb extension and retraction. Note that during zeiosis, no ethidium uptake is observed, i.e., there is little or no change in cell fluorescence. This result suggests that COP is not activated and the cells do not undergo a gross change in plasmalemmal permeability during zeiosis. At 1 nM MTX, the number of BAECs that undergo zeiosis in the presence of U73343 is increased (see Additional File 3). As seen in this movie (Additional File 3), the majority of the cells in the field of view (16 out of 24) undergo zeiosis, yet there is no ethidium uptake over the time frame examined, despite the higher concentration of MTX employed. Little or no zeiosis was observed in the absence of MTX, i.e., in the presence of either U73343 alone (4 zeotic cells out of 113) or vehicle alone (DMSO; 5 zeotic cells out of 146) examined for 40 min. Thus, the ability of MTX to cause zeiosis is specific, but requires the presence of U73343, presumably to block or prevent rapid oncotic cell death.

The cuvette experiments suggest that BAECs challenged with MTX can be rescued from oncotic cell death if U73343 is added to the bath solution within a narrow time frame after the addition of MTX. To further test this hypothesis, paired experiments were performed at the single cell level. BAECs, attached to coverslips were first challenged with MTX and subsequently rescued by addition of U73343. The percentage of a) dead cells (indicated by nuclear staining with ethidium), b) cells undergoing zeiosis, and c) surviving cells (indicated by the lack of membrane blebbing and lack of nuclear staining with ethidium) was quantified at time 40 min (Fig 6). All of the cells treated with vehicle alone (DMSO) before MTX exhibited the typical blebbing profile and nuclear staining indicative of rapid oncotic cell death. BAECs treated with U73343 before MTX were essentially protected from cell death, but ~35% of the total population exhibited zeiosis. The same pattern was observed when U73343 was added 4 min after MTX, i.e., full protection from oncosis with ~40% zeiosis. However, ~15% of the cells died by oncosis when U73343 was added at 6 min after MTX (see Additional File 4) and this percentage increased to >90% when

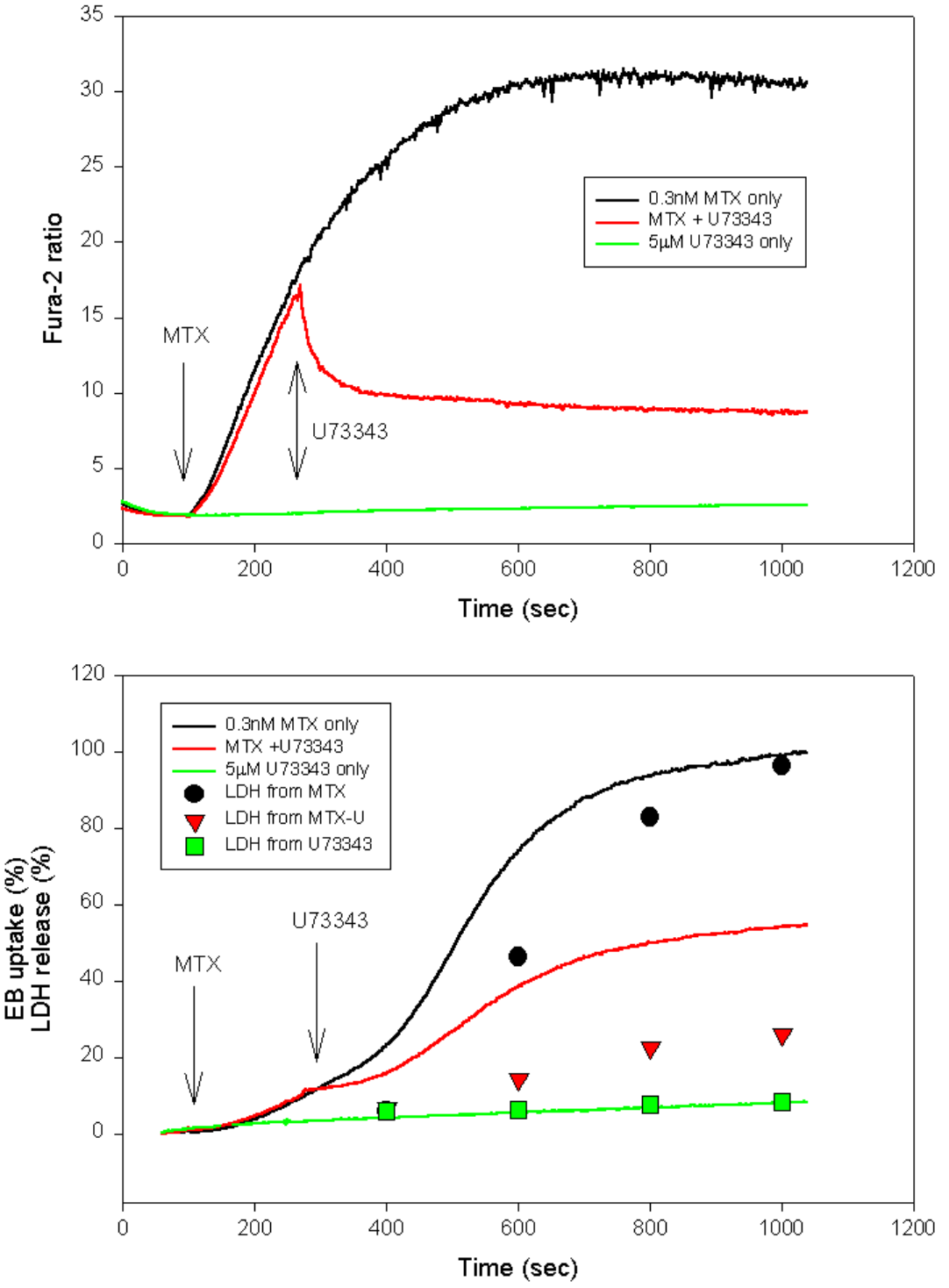

Figure 4
U73343 rescues the cells from MTX-induce lytic cell death. MTX-induced change in $[Ca^{2+}]_i$ (*upper panel*) or EB uptake (*lower panel*) were assayed in BAECs. MTX and U73343 were added at the concentrations and time indicated. LDH release was measured as described in *Materials and Methods* and plotted in the lower panel using color matched symbols (see *inset*). All experiments were performed in a paired fashion on the same batch of BAECs. Results shown are representative of 4 independent experiments.

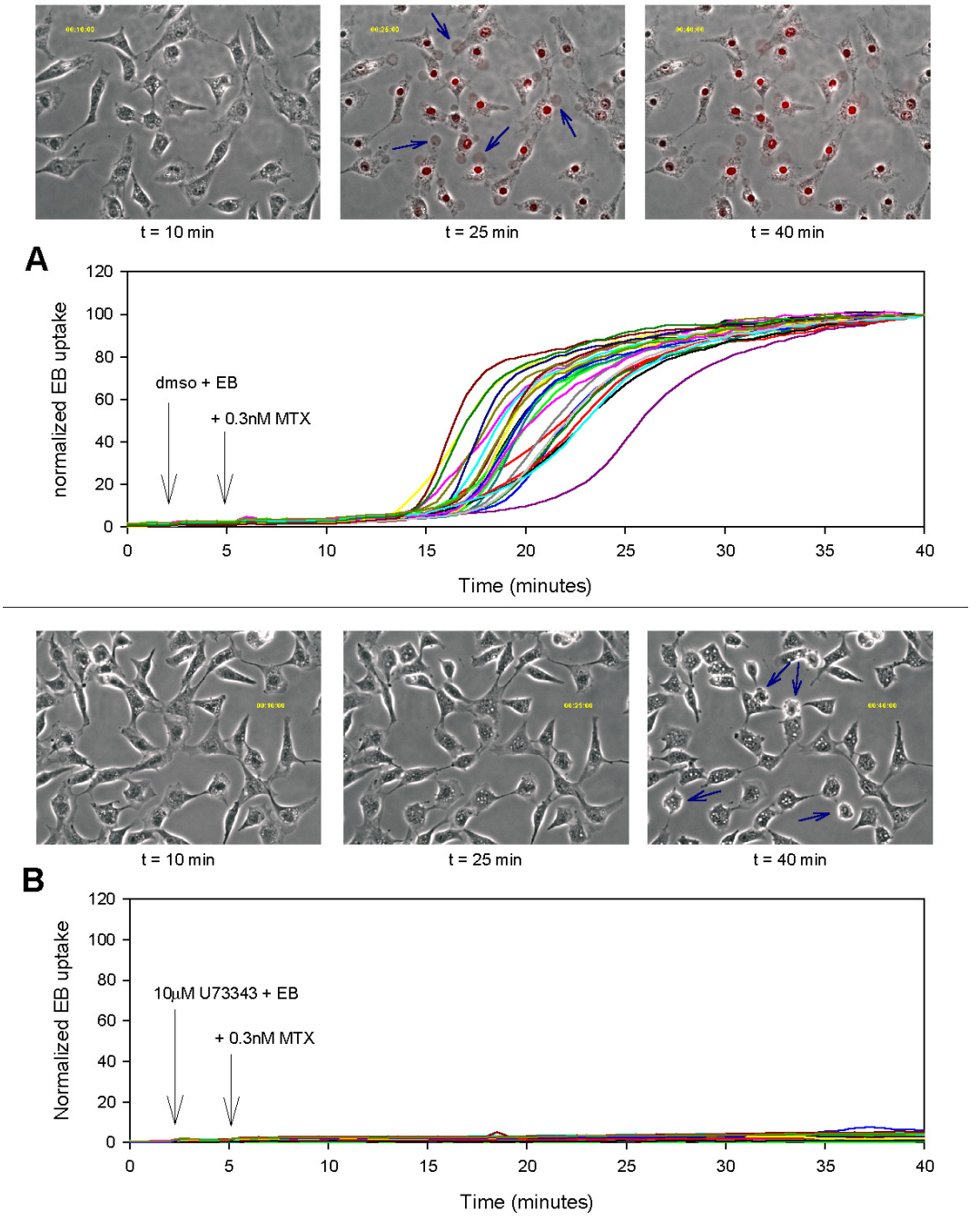

Figure 5
U73343 alters MTX-induced membrane blebbing. BAECs cultured on circular glass coverslips were visualized using an inverted microscope equipped for epifluorescence as described in *Materials and Methods.* The cells were maintained at 35–37°C and both phase and fluorescence images were acquired at 30-second intervals. The graph in each panel shows normalized single cell fluorescence intensity as a function of time for cells pretreated with either 0.2% DMSO (*Panel A;* n = 38) or U73343 (*Panel* B; n = 52) and subsequently challenged with MTX at the times indicated. Merged phase and fluorescence images (red pseudocolor) at time 10, 25, and 40 min are shown above each graph. Examples of large membrane blebs are highlighted by the blue arrows in *Panel A* at time 25 min. Examples of cells with rounded morphology are indicated by the blue arrows in *Panel B* at time 40 min. Note the absence of large dilated blebs and lack of fluorescence in the U73343-treated cells (*Panel B*). Results shown are representative of 9 and 6 independent experiments for *Panels A* and *B*, respectively.

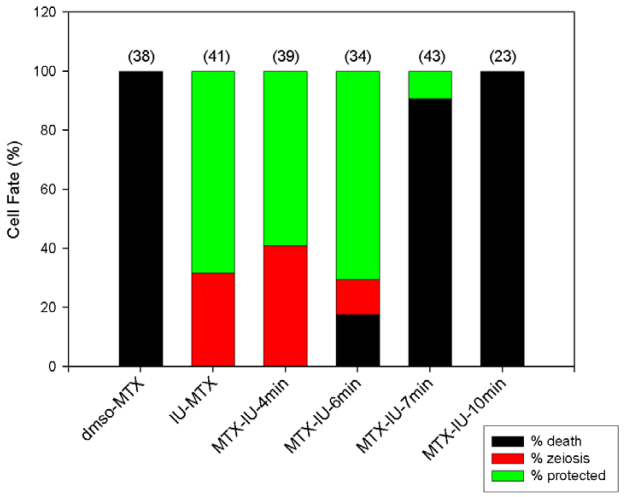

Figure 6
U73343 rescues BAECs from MTX-induce lytic cell death: Evaluation at the single cell level. BAECs, cultured on circular glass coverslips, were visualized using an inverted microscope equipped for epifluorescence as described in *Materials and Methods*. The cells were maintained at 35–37°C and both phase and fluorescence images were acquired at 30-sec intervals. Each bar of the histogram shows 1) the percentage of dead cells (black; indicated by uptake of ethidium and presence of large membrane blebs), 2) the percentage of cells undergoing zeiosis (red), and 3) the percentage of cells protected (green; indicated by the lack of nuclear staining and membrane blebbing) for the experimental condition given below each bar. The total number of cells examined for each condition is given in parenthesis above each bar. In each experiment 0.3 nM MTX was added at time 5 min; Bar 1, 0.2% DMSO added before MTX; bar 2, 10 μM U73343 added before MTX; bars 3, 4, 5, and 6, U73343 added 4, 6, 7, and 10 min after MTX, respectively. Percentages were determined at time 40 min using time-lapse videos to determine the number of cells undergoing zeiosis.

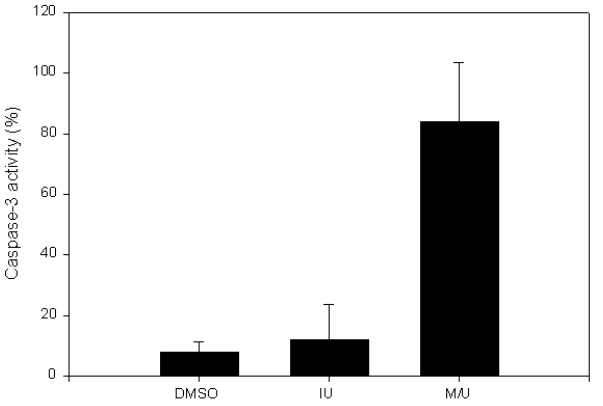

Figure 7
BAECs rescued from MTX-induced lytic cell death have elevated caspase-3 activity. BAECs were treated with 0.3 nM MTX for 2.5 min at which time the action of MTX was stopped by addition of 5 μM U73343. Cells were harvested after 48 hr and specific caspase-3 activity was determined using the fluorescence substrate assay (M/U). For control, caspase-3 activity was determined in cells treated with U73343 alone (IU) or vehicle (**DMSO**). Values represent the mean ± se (n = 3) relative to no-treatment controls.

U73343 was added at 7 min after MTX (see Additional File 5). Addition of U73343 10 min after MTX was the same as vehicle control, i.e., all the cells lyse by time 40 min. These results are consistent with the cuvette studies and directly demonstrate that within a narrow time window after MTX challenge, U73343 can rescue BAECs from oncotic cell death.

BAECs rescued from oncosis by U73343 die by apoptosis.
Zeiosis is a type of membrane blebbing associated with apoptosis [22–24]. Since U73343 protects cells from MTX-induced oncosis and causes zeiosis, we considered the possibility that the cells surviving the initial insult may ultimately die by apoptosis. To test this hypothesis, BAECs were treated with vehicle alone (DMSO), U73343 alone, or MTX followed by U73343, and specific caspase-3 activity was determined after 48 hrs by the fluorescence substrate assay (Fig 7). A significant increase in caspase-3 activity ($p < 0.035$; $n = 3$) was observed in cells challenged with MTX and subsequently rescued by U73343, consistent with increased apoptotic cell death.

Discussion
The results of the present study support two major conclusions. First, U73122 and U73343, compounds that are commonly used to examine PLC-dependent mechanisms, potently inhibit MTX-induced change in $[Ca^{2+}]_i$, vital dye uptake, and oncotic cell death in BAECs. The fact that U73343, which has essentially no effect on PLC at the concentrations employed [14,25–27], is more potent than U73122 on MTX-induced responses, clearly shows that the effect of these agents is unrelated to inhibition of PLC. Since U73343 can rapidly block and reverse the increase in $[Ca^{2+}]_i$ induced by MTX, it seems likely that these compounds directly block the MTX-activated channels in BAECs, perhaps acting as pore blockers. However, since the effect of U73343 appears to be slowly reversible, there may be additional sites/mechanisms of blocking action for these agents. Another class of compounds known as imidazoles, of which SKF 96365 is the best studied, have also been shown to block MTX-induced responses in many cell types [5,7,12,28]. The imidazoles, which are antifungal agents that inhibit cytochrome P_{450}, are relatively non-selective and are known to block voltage-gated Ca^{2+}

channels and receptor-activated Ca^{2+} influx through so-called store-operated channels (SOCs) [29], but their mechanism of action in this regard remains unknown.

U73343 appears to be relatively more selective than SKF 96365 with respect to Ca^{2+} influx pathways. Most studies find that U73343 has no effect on receptor-mediated increase in $[Ca^{2+}]_i$. However, Berven and Barritt [15] report that U73343 partially blocked vasopressin-induced Ca^{2+} influx, but did not inhibit release of Ca^{2+} from intracellular stores in hepatocytes. And Wang [16] reported that U73343 suppressed elevation of $[Ca^{2+}]_i$ in neutrophils challenged with FMLP in the presence, but not the absence, of extracellular Ca^{2+} Both reports are consistent with a lack of effect of U73343 on receptor-mediated activation of PLC and a direct inhibitory effect on Ca^{2+} influx pathways in these cells. The results of the present study therefore, suggest that the MTX-sensitive channel may be responsible for the rise in $[Ca^{2+}]_i$ produced by receptor stimulation in some cell types, but not in others. In this regard, Worley et al. [8] showed that SOCs in pancreatic β-cells have characteristics essentially identical to channels activated by MTX in the same cell type. Thus, U73343 may be useful for the ultimate identification and characterization of the physiological role of MTX-sensitive channels. Lastly, because MTX is one of the toxins associated with ciguatera seafood poisoning, the identification of U73343 as a potent and relatively specific blocker of MTX-induced cell death cascade may ultimately lead to improved therapeutic interventions.

The second major conclusion supported by the results of the present study is that MTX apparently has an effect on BAECs that is independent of the rise in $[Ca^{2+}]_i$. We previously showed that MTX causes the appearance of membrane blebs on the surface of the endothelial cells [3]. Initially these blebs are of small diameter (3–5 microns) and bleb formation correlates with the first phase of vital dye uptake. However, during MTX-induced cytolysis, as indicated by the release of LDH, the membrane blebs actually exhibit a dramatic increase in diameter. This bleb dilation phase is clearly associated with rapid, intense staining of the nucleus with vital dyes. It is well established that the acute effects of MTX on $[Ca^{2+}]_i$, uptake of vital dyes, and membrane blebbing require extracellular Ca^{2+}[1,3], but the role of cytosolic Ca^{2+} remains unknown. Preliminary studies in fibroblasts suggest that vital dye uptake via COP is attenuated in cells loaded with the Ca^{2+} chelator BAPTA [1], but the effect of BAPTA loading on MTX-induced bleb formation has not been examined. The results of the present study show that despite a blockade of MTX-induced change in $[Ca^{2+}]_i$, addition of U73343 either before, or within a short time after MTX, produced a blebbing profile known as zeiosis. The term zeiosis was first used by Costero and Pomerat [21] 50 years ago to describe the appearance of membrane vesicles on the surface of nerve cells in culture, as visualized using time-lapse cinematography. Although the cellular mechanisms remain poorly defined, it is now clear that zeiosis is associated with apoptotic cell death (for review [24,30]). In static images, the morphological changes associated with apoptosis appear as membrane blebs covering the surface of the cells [31–33]. However, time-lapse images reveal that blebs protrude and retract in a dynamic fashion, a hallmark of zeiosis [22,23]. Dynamic membrane blebbing appears to involve a dramatic change in the cytoskeleton and may be induced by a caspase-3-mediated cleavage of ROCK-I, a Rho-activated serine/threonine kinase known to stimulate actinomycin-based contractions [31–33]. A similar profile can be seen in the videos of MTX-induced cell death in the presence of U73343 (**Files 2 and 3**). The cells first lose adhesion to the coverslip, retract and roundup. This is followed by zeiotic membrane blebbing. Vital dyes are excluded during this time suggesting that COP is not activated and that there is no gross loss of membrane integrity during blebbing. It is important to note that these MTX-induced events are only observed in the presence of U73343 and occur in the absence of a measurable rise in $[Ca^{2+}]_i$. To our knowledge, this is the first evidence that MTX has effects independent of a rise in $[Ca^{2+}]_i$. Perhaps more importantly, the results of the present study suggest that U73343 converts MTX-induced oncosis into apoptosis and that a rise in $[Ca^{2+}]_i$ is necessary for oncotic cell death.

Conclusions

In conclusion, U73343 blocks the MTX-induced cell death cascade in BAECs and converts the normal blebbing profile seen with this toxin into zeiosis, a form of dynamic membrane blebbing commonly associated with apoptosis and characterized by bleb extension and retraction. U73343 may prove useful for identification and characterization of MTX-activated cation channels and for understanding their physiological role in cell signaling and cell death.

Materials and Methods

Solutions and reagents.

Unless otherwise indicated, HEPES-buffered saline (HBS) contained 140 mM NaCl, 5 mM KCl, 1 mM $MgCl_2$, 10 mM D-glucose, 1.8 mM $CaCl_2$, 15 mM HEPES, 0.1% bovine serum albumin, pH adjusted to 7.40 at 37°C with NaOH. Fura-2 acetoxymethyl ester (fura-2/AM) and ethidium bromide (EB) were obtained from Molecular Probes (Eugene, OR, USA). Maitotoxin (MTX), obtained from LC Laboratories (Woburn, MA) or Wako Bioproducts (Richmond, VA), was stored as a stock solution in ethanol at -20°C. All other salts and chemicals were of reagent grade.

Cell Culture.
Bovine aortic endothelial cells were cultured as previously described [34] using Dulbecco's modified Eagles medium (GIBCO) supplemented with 10% fetal bovine serum (Hyclone, Logan UT), 100 μg/ml streptomycin and 100 μg/ml penicillin (complete-DMEM). All cultures demonstrated contact-inhibited cobblestone appearance typical of endothelial cells grown to confluence.

Measurement of the apparent cytosolic free Ca^{2+} concentration.
$[Ca^{2+}]_i$ was measured using the fluorescent indicator, fura-2, as previously described [35]. Experiments were performed with cells in the twelfth to twentieth passage and 2–3 days post-confluency. Briefly, cells were harvested and re-suspended in HBS containing 20 μM fura-2/AM. Following 30 min incubation at 37°C, the cell suspension was diluted ~10-fold with HBS, incubated for an additional 30 min, washed and resuspended in fresh HBS. Aliquots from this final suspension were subjected to centrifugation and washed twice immediately prior to fluorescence measurement. Fluorescence was recorded using an SLM 8100 spectrophotofluorometer; excitation wavelength alternated between 340 and 380 nm and fluorescence intensity was monitored at an emission wavelength of 510 nm. All measurements were performed at 37°C.

Measurement of vital dye uptake.
Vital dye uptake was determined as previously described [1–3]. Briefly, an aliquot (2 ml) of dispersed cells suspended in HBS at 37°C was placed in a cuvette. Following addition of ethidium bromide (final concentrations of 5 μM), fluorescence was recorded as a function of time with excitation and emission wavelengths of 302/560 nm, respectively. All ethidium bromide fluorescence values were corrected for background (extracellular) dye fluorescence and expressed as a percentage relative to the value obtained following complete permeabilization of the cells with 50 μM digitonin.

For single cell measurement of vital dye uptake, BAECs in complete-DMEM were sparsely seeded on circular glass coverslips and used within 2–3 days of seeding. The coverslips were mounted in temperature-controlled perfusion chambers and placed on the stage of Nikon Diaphot inverted microscope. The cells were illuminated with light from a 75 watt xenon lamp using a 0–5722 filter cube obtained from Molecular Probes. Epifluorescence was recorded using a SPOT™ camera (Diagnostic Instruments, Sterling Heights, MI) and images were acquired and analyzed using SimplePCI imaging software (Compix Inc., Cranberry Township, PA). During each experiment, phase and fluorescence image pairs were collected at 30 second intervals with shutter controllers switching between light and fluorescent illumination. The fluorescence images were used to quantify dye uptake. A region over the nucleus of individual cells was defined and the average fluorescence intensity of the region was quantified as a function of time. Phase images were contrast enhanced, digitally merged with the corresponding fluorescent images, and time-lapse videos were created using the SimplePCI software.

Measurement of lactate dehydrogenase (LDH) release.
Aliquots of dispersed cells (2 ml) were incubated at 37°C for various lengths of time in the presence and absence of MTX. The cells were pelleted by centrifugation for 15 sec at 12,000 rpm in an Eppendorf centrifuge (model 5415 C). The supernatants were removed, and placed on ice. Enzyme activity in aliquots (50 μl) of the supernatants was determined using the LD-L kit from Sigma. All values are expressed as percent LDH released relative to the value obtained following permeabilization of the cells with 50 μM digitonin.

Measurement of specific caspase-3 activity.
Extracts were obtained from confluent BAECs following the indicated treatment using a freeze-thaw lysis protocol. BAECs were mechanically harvested, washed, and resuspended in 500 μl lysis buffer (10 mM Tris pH 7.5, 100 mM NaCl, 1 mM EDTA, 0.01% Triton X-100). The cell suspension was frozen using liquid nitrogen and rapidly thawed in a 37°C water bath. Following 5 freeze-thaw cycles, the cell suspensions were subjected to centrifugation for 5 min at 5000 rpm at 4°C in an Eppendorf 5417R centrifuge. Supernatants were collected and stored at -20°C. Protein concentration was determined by the method of Lowry using bovine serum albumin as standard. Cytosolic extracts (300 μg protein) were assayed for caspase-3 activity according to the protocol described in the EnzChek Caspase-3 Assay Kit (Molecular Probes). Specific caspase-3 activity, defined as the activity inhibitable by Ac-DEVD-CHO, was normalized to that of untreated BAECs.

Additional material

Additional file 1

MTX-induced EB uptake and membrane blebbing in single BAECs. The time-lapse video of the experiment shown in Fig 5A was created from the captured images as described in Material and Methods, with a time compression of 3.5 min (i.e., 7 images) per second. The phase and EB fluorescence images, taken every 30 sec for 40 min, were merged into a single video with EB fluorescence shown as red pseudocolor.
Click here for file
[http://www.biomedcentral.com/content/supplementary/1472-6793-2-2-S1.avi]

Additional file 2

Effect of U73343 pretreatment on MTX-induced EB uptake and membrane blebbing in single BAECs. The time-lapse video of the experiment shown in Fig 5B was created from the captured images as described in Material and Methods, with a time compression of 3.5 min (i.e., 7 images) per second. The phase and EB fluorescence images, taken every 30 sec for 40 min, were merged into a single video with EB fluorescence shown as red pseudocolor.
Click here for file
[http://www.biomedcentral.com/content/supplementary/1472-6793-2-2-S2.avi]

Additional file 3

Zeiosis induced by a high concentration of MTX. The effect of 1 nM MTX on ethidium uptake and membrane blebbing in the presence of U73343 (10 μM) was performed as described in the legend for Fig. 5B. The time-lapse video was created from the captured images as described in Material and Methods, with a time compression of 3.5 min (i.e., 7 images) per second. The phase and EB fluorescence images, taken every 30 sec for 60 min, were merged into a single video with EB fluorescence shown as red pseudocolor.
Click here for file
[http://www.biomedcentral.com/content/supplementary/1472-6793-2-2-S3.avi]

Additional file 4

Rescue of MTX-treated cells by U73343. Time-lapse video for the experiment described in Fig 6 with U73343 added at 6 min after MTX, was created from the captured images as described in Material and Methods, with a time compression of 3.5 min (i.e., 7 images) per second. The phase and EB fluorescence images, taken every 30 sec for 40 min, were merged into a single video with EB fluorescence shown as red pseudocolor.
Click here for file
[http://www.biomedcentral.com/content/supplementary/1472-6793-2-2-S4.avi]

Additional file 5

Rescue of MTX-treated cells by U73343. Time-lapse video for the experiment described in Fig 6 with U73343 added at 7 min after MTX, was created from the captured images as described in Material and Methods, with a time compression of 3.5 min (i.e., 7 images) per second. The phase and EB fluorescence images, taken every 30 sec for 40 min, were merged into a single video with EB fluorescence shown as red pseudocolor.
Click here for file
[http://www.biomedcentral.com/content/supplementary/1472-6793-2-2-S5.avi]

Acknowledgements

We thank Zack Novince and Justin Weinberg for excellent technical assistance. This work was supported in part by NIH grant GM52019 and grant 9950014N from the National American Heart Association.

References

1. Schilling WP, Sinkins WG, Estacion M: **Maitotoxin activates a non-selective cation channel and a P2Z/P2X$_7$-like cytolytic pore in human skin fibroblasts.** *Am J Physiol* 1999, **277**:C755-C765
2. Schilling WP, Wasylyna T, Dubyak GR, Humphreys BD, Sinkins WG: **Maitotoxin and P2Z/P2X7 purinergic receptor stimulation activates a common cytolytic pore.** *Am J Physiol* 1999, **277**:C766-C776
3. Estacion M, Schilling WP: **Maitotoxin-induced membrane blebbing and cell death in bovine aortic endothelial cells.** *BMC Physiology* 2001, **1**:2
4. Bielfeld-Ackermann A, Range C, Korbmacher C: **Maitotoxin (MTX) activates a non-selective cation channel in *Xenopus laevis* oocytes.** *Pflugers Arch* 1998, **436**:329-337
5. Dietl P, Völkl H: **Maitotoxin activates a nonselective cation channel and stimulates Ca^{2+} entry in MDCK renal epithelial cells.** *Mol Pharmacol* 1994, **45**:300-305
6. Estacion M, Nguyen HB, Gargus JJ: **Calcium is permeable through a maitotoxin-activated nonselective cation channel in mouse L cells.** *Am J Physiol Cell Physiol* 1996, **270**:C1145-C1152
7. Musgrave IF, Seifert R, Schultz G: **Maitotoxin activates cation channels distinct from the receptor-activated non-selective cation channels of HL-60 cells.** *Biochem J* 1994, **301**:437-441
8. Worley JF III, McIntyre MS, Spencer B, Dukes ID: **Depletion of intracellular Ca^{2+} stores activates a maitotoxin-sensitive non-selective cationic current in β-cells.** *J Biol Chem* 1994, **269**:32055-32058
9. Nishio M, Muramatsu I, Yasumoto T: **Na$^+$-permeable channels induced by maitotoxin in guinea-pig single ventricular cells.** *Eur J Pharmacol* 1996, **297**:293-298
10. Faivre JF, Deroubaix E, Coulombe A, Legrand AM, Coraboeuf E: **Effect of maitotoxin on calcium current and background inward current in isolated ventricular myocytes.** *Toxicon* 1990, **28**:925-937
11. Kobayoshi M, Ochi R, Ohizumi Y: **Maitotoxin-activated single calcium channels in guinea-pig cardiac cells.** *Br J Pharmacol* 1987, **92**:665-671
12. Soergel DG, Yasumoto T, Daly JW, Gusovsky F: **Maitotoxin effects are blocked by SK&F 96365 an inhibitor of receptor-mediated calcium entry.** *Mol Pharmacol* 1992, **41**:487-493
13. Gusovsky F, Daly JW: **Maitotoxin: a unique pharmacological tool for research on calcium-dependent mechanisms.** *Biochem Pharmac* 1990, **39**:1633-1639
14. Smith RJ, Sam LM, Justen JM, Bundy GL, Bala GA, Bleasdale JE: **Receptor-coupled signal transduction in human polymorphonuclear neutrophils: Effects of a novel inhibitor of phospholipase C-dependent processes on cell responsiveness.** *J Pharmacol Exp Ther* 1990, **253**:688-697
15. Berven LA, Barritt GJ: **Evidence obtained using single hepatocytes for inhibition by the phospholipase C inhibitor U73122 of store-operated Ca^{2+} inflow.** *Biochem Pharmacol* 1995, **49**:1373-1379
16. Wang JP: **U-73122 an aminosteroid phospholipase C inhibitor, may also block Ca^{2+} influx through phospholipase C-independent mechanism in neutrophil activation.** *Naunyn Schmiedebergs Arch Pharmacol* 1996, **353**:599-605
17. Taylor CW, Broad LM: **Pharmacological analysis of intracellular Ca^{2+} signalling: problems and pitfalls.** *TIPS* 1998, **19**:370-375
18. Bosch RR, Patel AM, Van Emst-De Vries SE, Smeets RL, De Pont JJ, Willems PH: **U73122 and U73343 inhibit receptor-mediated phospholipase D activition downstream of phospholipase C in CHO cells.** *Eur J Pharmacol* 1998, **346**:345-351
19. Heemskerk JW, Feijge MA, Sage SO, Farndale RW: **Human platelet activation is inhibited upstream of the activation of phospholipase A2 by U73343.** *Biochem Pharmacol* 1997, **53**:1257-1262
20. Hildebrandt JP, Plant TD, Meves H: **The effects of bradykinin on K$^+$ currents in NG108-15 cells treated with U73122 a phospholipase C inhibitor, or neomycin.** *Br J Pharmacol* 1990, **120**:841-850

21. Costero I, Pomerat CM: **Cultivation of neurons from the adult human cerebral and cerebellar cortex.** *Am J Anat* 1951, **89**:405-467
22. Shotton DM, Attaran A: **Variant antigenic peptide promotes cytotoxic T lymphocyte adhesion to target cells without cytotoxicity.** *Proc Natl Acad Sci USA* 1998, **95**:15571-15576
23. Lowy RJ, Dimitrov DS: **Characterization of influenza virus-induced death of J774.1 macrophages.** *Exp Cell Res* 1997, **234**:249-258
24. Mills JC, Stone NL, Pittman RN: **Extranuclear apoptosis: The role of the cytoplasm in the execution phase.** *J Cell Biol* 1999, **146**:703-707
25. Yule DI, Williams JA: **U73122 inhibits Ca^{2+} oscillations in response to cholecystokinin and carbachol but not to JMV-180 in rat pancreatic acinar cells.** *J Biol Chem* 1992, **267**:13830-13835
26. Thompson AK, Mostafapour SP, Denlinger LC, Bleasdale JE, Fisher SK: **The aminosteriod U-73122 inhibits muscarinic receptor sequestration and phosphoinositide hydrolysis in SK-N-SH neuroblastoma cells.** *J Biol Chem* 1991, **266**:23856-23862
27. Bleasdale JE, Thakur NR, Gremban RS, Bundy GL, Fitzpatrick FA, Smith RJ, *et al*: **Selective inhibition of receptor-coupled phospholipase C-dependent processes in human platelets and polymorphonuclear neutorphils.** *J Pharmacol Exp Ther* 1990, **255**:756-768
28. Daly JW, Lueders J, Padgett WL, Shin Y, Gusovsky F: **Maitotoxin-elicited calcium influx in cultured cells effect – Effect of calcium-channel blockers.** *Biochem Pharmacol* 1995, **50**:1187-1197
29. Merritt JE, Armstrong WP, Benham CD, Hallam TJ, Jacob R, Jaxa-Chamiec A, *et al*: **SK&F 96365 a novel inhibitor of receptor-mediated calcium entry.** *Biochem J* 1990, **271**:515-522
30. Willingham MC: **Cytochemical methods for the detection of apoptosis.** *J Histochem Cytochem* 1999, **47**:1101-1109
31. Leverrier Y, Ridley AJ: **Apoptosis: caspases orchestrate the ROCK 'n' bleb.** *Nature Cell Biology* 2001, **3**:E91-E93
32. Coleman ML, Sahai EA, Yeo M, Bosch M, Dewar A, Olson MF: **Membrane blebbing during apoptosis results from caspase-mediated activation of ROCK I.** *Nature Cell Biology* 2001, **3**:339-345
33. Sebbagh M, Renvoizé C, Hamelin J, Riché N, Bertoglio J, Bréard J: **Caspase-3-mediated cleavage of ROCK I induces MLC phosphorylation and apoptotic membrane blebbing.** *Nature Cell Biology* 2001, **3**:346-352
34. Eskin SG, Sybers HD, Trevino L, Lie JT, Chimoskey JE: **Comparison of tissue-cultured bovine endothelial cells from aorta and saphenous vein.** *In vitro* 1978, **14**:903-910
35. Schilling WP, Rajan L, Strobl-Jager E: **Characterization of the bradykinin-stimulated calcium influx pathway of cultured vascular endothelial cells: Saturability, selectivity and kinetics.** *J Biol Chem* 1989, **264**:12838-12848